JTE HCMUTE
ISSN: 2615-9740

JOURNAL OF TECHNICAL EDUCATION SCIENCE
Ho Chi Minh City University of Technology and Education
Website: https://jte.edu.vn
Email: jte@hcmute.edu.vn

Intelligent Control System based on Wavelet Type-2 Fuzzy Neural network Design For Robot System

Duc-Hung Pham
Hung Yen University of Technology and Education, Hung Yen, Vietnam
Corresponding author. *Email: duchung.pham@utehy.edu.vn*

ARTICLE INFO

Received:	09/01/2024
Revised:	20/03/2024
Accepted:	29/03/2024
Published:	28/04/2024

KEYWORDS

Wavelet function;
Type-2 fuzzy system;
Brain imitated controller;
Two-joint robot manipulator;
Sliding mode control.

ABSTRACT

In this paper, we propose a wavelet type-2 fuzzy brain imitated controller (WT2FBIC) for nonlinear robotic systems. The suggested method combines a wavelet type-2 fuzzy system (WT2FS) and a brain imitated controller (BIC) to improve learning efficiency. The system's inputs, which comprise a sensory and an emotional channel, eventually lead to the network's output. The WT2FBIC parameter update rules use the Lyapunov theory and the gradient descent method. To correct for the WT2FBIC in a main controller, a robust controller can be used for compensation. Robots find applications in a wide variety of industries thus the proposed WT2FBIC-based control system is used to control nonlinear robotic systems. In this work, a two-jointed robotic manipulator control system used the proposed method is demonstrated. The comparison of the proposed method with recent methods point out the effectiveness of the proposed method. The simulation results indicate that the proposed control approach provides good control performance.

Doi: https://doi.org/10.54644/jte.2024.1519

1. Introduction

Robots find applications in a wide variety of industries, including those pertaining to flight [1], healthcare [1], robot collaboration and cooperation [2], and surgery [3], [4]. The following are some examples of applications that fall under this category: An example of a highly coupled nonlinear dynamic multi-input-multi-output (MIMO) system with undetermined system parameters is a robotic manipulator, which is also known as a robotic arm. It is of the utmost importance that each of the angular positions of the joint be in the appropriate location, in accordance with the target position that has been specified for the joint.

In recent years, numerous researchers in the field of control have shown an increasing interest in biologically inspired algorithms such as fuzzy sets, neural networks [5] to solve challenging optimization and control problems. As a direct result of the recent development of a mathematical model for emotional learning in a relatively insignificant region of the human brain, the amygdala, a brand new scientific subfield known as biologically motivated systems has recently emerged [6]. Researchers in experimental psychology, artificial intelligence (AI) and cognitive science have long been aware of the interaction between a person's thoughts and feelings.

This is due to the inaccuracy caused by system uncertainties and external disturbances. The Brain Imitated Controller (BIC) was developed by Lucas and his colleagues [6] in an effort to find answers to these problems. BIC is composed of six different components: emotional input, emotional learning, emotional output, controller output and sensory input. BIC has been integrated with a new system to improve the overall functionality of the platform, such as the Cerebellar Model Articulation Controller [7], the Takagi-Sugeno-Kang fuzzy system [8].

A robust controller is required to address nonlinearity and uncertainty. The most common control algorithm is a robust control algorithm [9], [10]. Therefore, a robust controller is implemented in the proposed control system to make it stable. Robust control system has been applied for various nonlinear systems, such as missile guidance control [10], robot system [11], [12], [13], and fault tolerant control [14]. The robust controller also acts as the compensator to make the control system come to stable better.

Sliding mode control (SMC) is a powerful method that can control both non-linear and linear systems and has recently been the subject of intensive research by scientists worldwide. The SMC is characterized by its robustness, stability, good transient response and fast output response. In addition, the control technology is uncomplicated and easy to use in practice. For these reasons, the SMC is implementing in this study.

In this work, a combination of a wavelet type 2 fuzzy system and a BIC is created. The new controller is called Wavelet Type 2 fuzzy brain imitated controller (WT2FBIC). The WT2BBIC is used to control a two-jointed robotic manipulator.

The main contributions of this paper can be listed as follows:

a) A new WT2FBC is created and parameter of the WT2FBC is updated online by using the gradient descent method.
b) The system stability is proven by Lyapunov theory.
c) The proposed control system is applied for a two-joint robot manipulator.
d) The comparisons of the proposed method with recent methods point out the effectiveness of WT2FBC.

The content of this paper can be structured as follows: section 2 presents the problem formulation, section 3 shows the structure of the proposed method, section 4 presents the parameters and specification for online learning of the proposed method. Section 4 introduces the simulation results, and finally section 6 summarizes the conclusions and future directions.

2. Problem Formulation

The formulation of a nonlinear system can be demonstrated in the following:

$$\boldsymbol{\chi}^{(n)} = \boldsymbol{f}(\boldsymbol{\chi})) + \boldsymbol{G}(\boldsymbol{\chi})\boldsymbol{u} + \boldsymbol{l}(\boldsymbol{\chi}) \tag{1}$$

where $\boldsymbol{f}(\boldsymbol{\chi})$ and $\boldsymbol{G}(\boldsymbol{\chi})$ are nonlinear uncertain functions. $\boldsymbol{l}(\boldsymbol{\chi}) = [l_1, l_2, ..., l_m]^T \in \Re^m$ is the lumped uncertainty of the system, $\boldsymbol{u} = [u_1, u_2, ..., u_m]^T \in \Re^m$ is control signal and $\boldsymbol{\chi} = [\chi_1, \chi_2, ..., \chi_m]^T \in \Re^m$. In the case that one disregards the possibility of uncertainty as well as other kinds of influence of the external disturbance, the nominal system of (1) can be expressed as follows:

$$\boldsymbol{\chi}^{(n)} = \boldsymbol{f}_0(\boldsymbol{\chi}) + \boldsymbol{G}_0(\boldsymbol{\chi})\boldsymbol{u} \tag{2}$$

where $\boldsymbol{G}_0 = diag(g_{01}, g_{02}, \cdots, g_{0m})$ and $\boldsymbol{f}_0(\boldsymbol{\chi})$ are the nominal parts of $\boldsymbol{G}$ and $\boldsymbol{f}$, respectively. Without losing generality, it is assumed that $g_{0i} \geq 0$ for $i = 1, \cdots, m.$ It is also assumed that the nonlinear system of (2) is controllable and that $\boldsymbol{G}_0^{-1}$ exists. Then, the nonlinear system (1) can be described as

$$\boldsymbol{\chi}^{(n)} = \boldsymbol{f}_0 + \boldsymbol{G}_0\boldsymbol{u} + \boldsymbol{l}(\boldsymbol{\chi}) \tag{3}$$

where the lumped uncertainty is specified as $\boldsymbol{l}(\boldsymbol{\chi})$, taking into account not only the system's inherent uncertainties but also any outside disturbances. The task of designing an appropriate control system so that the output $\boldsymbol{\chi}$ of the system can follow a desired trajectory vector $\boldsymbol{\chi}_r = [\chi_{r1}, \chi_{r2}, ..., \chi_{rm}]^T \in \Re^m$. The tracking error can be defined as

$$\boldsymbol{e} \equiv \boldsymbol{\chi}_r - \boldsymbol{\chi} \tag{4}$$

If all of these factors $\boldsymbol{f}_0$, $\boldsymbol{G}_0$ and $\boldsymbol{l}(\boldsymbol{\chi})$ are exactly known, then it will be possible to design the perfect controller as

$$\boldsymbol{u}^* = \boldsymbol{G}_0^{-1}\left(\boldsymbol{\chi}_r^{(n)} - \boldsymbol{f}_0(\boldsymbol{\chi}) - \boldsymbol{l}(\boldsymbol{\chi}) + \Gamma^T\boldsymbol{e}\right) \tag{5}$$

where $\Gamma = \left[\Gamma_m, ..., \Gamma_2, \Gamma_1\right]^T$ are the feedback gain matrix that have positive values. By inserting the ideal controller into equation (3), one can obtain the dynamic error equation

$$\boldsymbol{e}^{(n)} + \Gamma^T \times \boldsymbol{e} = 0 \tag{6}$$

In the event that Γ is selected to be a Hurwitz polynomial, it suggests that $\lim_{t\to\infty}\|\boldsymbol{e}\|=0$. However, $\boldsymbol{l}(\chi)$ cannot be identified in practical applications, so $\boldsymbol{u}^*$ is not available. Therefore, a wavelet type-2 fuzzy brain imitated controller (WT2FBIC) can be planned to imitator $\boldsymbol{u}^*$.

3. The structure of proposed method

The proposed WT2FBIC (Figure 1) comprises five spaces: Input space, sensory cortex space, weight space, amygdala and orbitofrontal cortex space and output space.

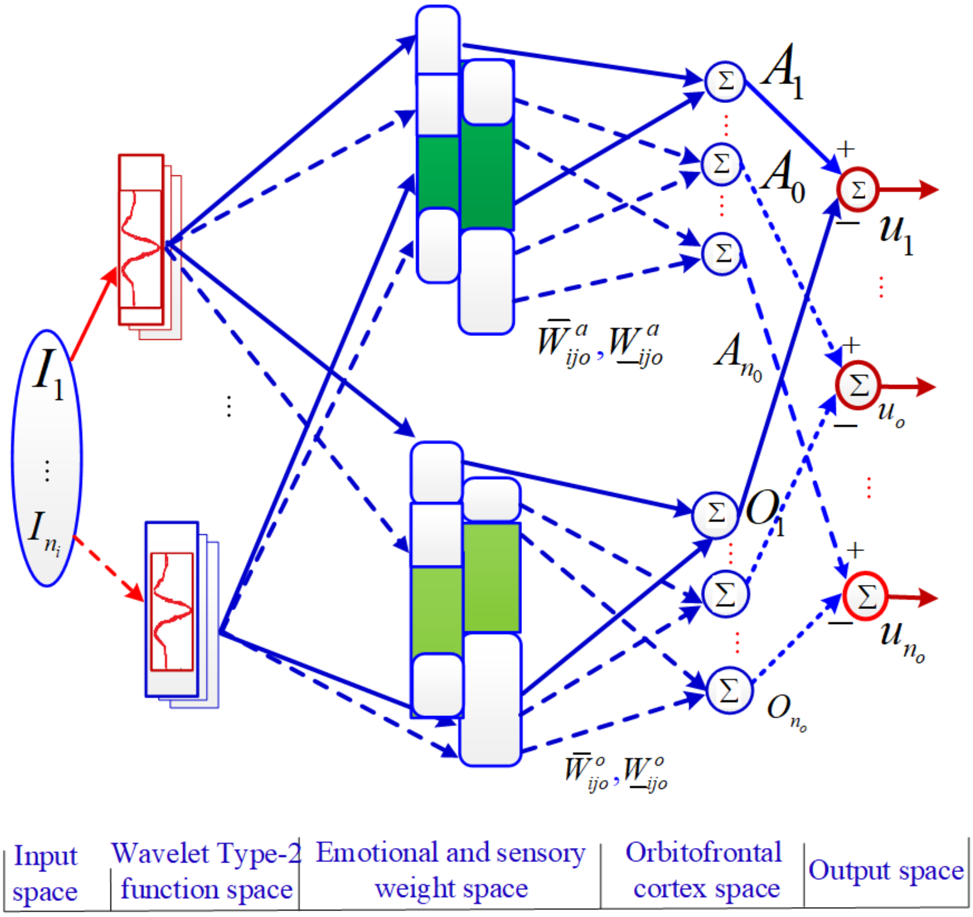

Figure 1. *The structure of WT2FBIC*

3.1. Space 1: Input

$\boldsymbol{I}=\left\lfloor I_1, I_2,\ldots,I_{n_i}\right\rfloor \in R^{n_i}$, n_i is the input's dimension. Two-channel WT2FBIC using the orbitofrontal cortex and the amygdala. When it comes to making decisions based on feelings, the amygdala channel is involved, whereas the orbitofrontal cortex channel is used for emotional control. One way to describe fuzzy rules is as follows:

If I_1 is S_{1j} and I_2 is S_{2j}... and I_{n_i} *is* S_{n_i} then $A_o = W^a_{ijo}$ and $O_o = W^o_{ijo}$, for j=1,2,...,n_j; $o=1,2,\ldots,n_o$. (7)

where S_{ij} is the fuzzy set connected the *i*-th input to the *j*-th space; n_j, n_i, and n_o are respectively the dimension of layer space, input space, and output space; O_o, A_o are orbitofrontal and amygdala channel, respectively.

3.2. Sensory cortex space

First, let set:

$$\bar{P}_{ij} = \frac{I_i - \mu_{ij}}{\bar{v}_{ij}} \tag{8}$$

where μ_{ij} and $\bar{v}_{ij}$ are respectively the center and upper dilation. Upper wavelet function is given as follows

$$\bar{S}_{ij} = -\bar{P}_{ij}^2 e^{(-\frac{1}{2}\bar{P}_{ij}^2)} \tag{9}$$

where μ_{ij} and $\underline{v}_{ij}$ are respectively the center and lower dilation. Lower wavelet function is given as follows

$$\underline{P}_{ij} = \frac{I_i - \mu_{ij}}{\underline{v}_{ij}} \tag{10}$$

$$\underline{S}_{ij} = -\underline{P}_{ij}^2 e^{(-\frac{1}{2}\underline{P}_{ij}^2)} \tag{11}$$

3.3. Weight space

Upper and lower weights of sensory and emotional are $\bar{W}_{ijo}^a$, $\underline{W}_{ijo}^a$, $\bar{W}_{ijo}^o$ and $\underline{W}_{ijo}^o$, respectively.

3.4. Amygdala and orbitofrontal cortex space

$$A_o = \frac{1}{2} \times \left(\frac{\sum_{i=1}^{n_i}\sum_{j=1}^{n_j} S_{ij}^l \underline{W}_{ijo}^a}{\sum_{i=1}^{n_i}\sum_{j=1}^{n_j} S_{ij}^l} + \frac{\sum_{i=1}^{n_i}\sum_{j=1}^{n_j} S_{ij}^r \bar{W}_{ijo}^a}{\sum_{i=1}^{n_i}\sum_{j=1}^{n_j} S_{ij}^r} \right) \tag{12}$$

$$O_o = \frac{1}{2} \times \left(\frac{\sum_{i=1}^{n_i}\sum_{j=1}^{n_j} S_{ij}^l \underline{W}_{ijo}^o}{\sum_{i=1}^{n_i}\sum_{j=1}^{n_j} S_{ij}^l} + \frac{\sum_{i=1}^{n_i}\sum_{j=1}^{n_j} S_{ij}^r \bar{W}_{ijo}^o}{\sum_{i=1}^{n_i}\sum_{j=1}^{n_j} S_{ij}^r} \right) \tag{13}$$

The calculation of the reduction from type-2 to type-1 with the Karnik-Mendel algorithm, as shown in [9], is possible.

$$S_{ij}^l = \begin{cases} \underline{S}_{ij}, & j > L \\ \bar{S}_{ij}, & \text{others} \end{cases} \tag{14}$$

$$S_{ij}^r = \begin{cases} \bar{S}_{ij}, & j > R \\ \underline{S}_{ij}, & \text{others} \end{cases} \tag{15}$$

where R and L are the right and left switching point.

3.5. Output space

The o-th output of WT2FBIC could be caculated as

$$u_o = A_o - O_o \tag{16}$$

Then the output of proposed controller can be calculated as follows

$$\boldsymbol{u}_{WT2FBIC} = \sum_{o=1}^{n_o} \left(A_o - O_o \right) \tag{17}$$

4. Parameters and specifications for online learning of the WT2FBIC

A cost function is selected as the

$$F_{\text{cost}} = \frac{1}{2}\sum_{o=1}^{n_o}(d_o - u_o)^2 \tag{18}$$

where d_o is the desired control output. The formula for updating the parameters can be derived as

$$\vartheta(t+1) = \vartheta(t) + \Delta\vartheta(t) = \vartheta(t) - \lambda_\vartheta \frac{\partial F_{\text{cost}}(t)}{\partial \vartheta} \tag{19}$$

where ϑ can be one of these variables $\mu_{ij}, \underline{v}_{ij}$ or $\overline{v}_{ij}$. λ_ϑ are the learning rates. According to the structure of the proposed controller in figure 1, the cost function and by using the chain rule and gradient descent method, the parameters updating can be holded as follows [10].

$$\begin{aligned}\Delta\mu_{ij} &= -\lambda_\mu \frac{\partial \Omega(t)}{\partial \mu_{ij}} = -\lambda_\mu \frac{\partial \Omega(t)}{\partial u_o}\left(\frac{\partial u_o}{\partial \underline{S}_{ij}}\frac{\partial \underline{S}_{ij}}{\partial \underline{F}_{ij}}\frac{\partial \underline{F}_{ij}}{\partial \mu_{ij}} + \frac{\partial u_o}{\partial \overline{S}_{ij}}\frac{\partial \overline{S}_{ij}}{\partial \overline{F}_{ij}}\frac{\partial \overline{F}_{ij}}{\partial \mu_{ij}}\right) \\ &= \lambda_\mu \times \left((\underline{W}_{ijo}^a - \underline{W}_{ijo}^o)(-\underline{F})e^{(\frac{-\underline{F}^2}{2})}\left(2-\underline{F}^2\right)\frac{\underline{F}}{I_i - \mu_{ij}} + (\overline{W}_{ijo}^a - \overline{W}_{ijo}^o)(-\overline{F})e^{(\frac{-\overline{F}^2}{2})}\left(2-\overline{F}^2\right)\frac{\overline{F}}{I_i - \mu_{ij}}\right) \\ &= \lambda_\mu \left((\underline{W}_{ijo}^a - \underline{W}_{ijo}^o)\left(-\underline{F}^2 e^{(-\frac{\underline{F}^2}{2})}\right)\frac{\left(2-\underline{F}^2\right)}{I_i - \mu_{ij}} + (\overline{W}_{ijo}^a - \overline{W}_{ijo}^o)\left(-\overline{F}^2 e^{(-\frac{\overline{F}^2}{2})}\right)\frac{\left(2-\overline{F}^2\right)}{I_i - \mu_{ij}}\right)\end{aligned} \tag{20}$$

$$\Rightarrow \Delta\mu_{ij} = \lambda_\mu \left((\underline{W}_{ijo}^a - \underline{W}_{ijo}^o)\underline{S}_{ij}\frac{\left(2-\underline{F}^2\right)}{I_i - \mu_{ij}} + (\overline{W}_{ijo}^a - \overline{W}_{ijo}^o)\overline{S}_{ij}\frac{\left(2-\overline{F}^2\right)}{I_i - \mu_{ij}}\right) \tag{21}$$

$$\Delta\underline{v}_{ij} = -\lambda_{\underline{v}}\frac{\partial \Omega(t)}{\partial \underline{v}_{ij}} = -\lambda_{\underline{v}}\frac{\partial \Omega(t)}{\partial u_o}\left(\frac{\partial u_o}{\partial \underline{S}_{ij}}\frac{\partial \underline{S}_{ij}}{\partial \underline{v}_{ij}} + \frac{\partial u_o}{\partial \overline{S}_{ij}}\frac{\partial \overline{S}_{ij}}{\partial \underline{v}_{ij}}\right) = \lambda_{\underline{v}}\sum_{o=1}^{n_o}(\underline{W}_{ijo}^a - \underline{W}_{ijo}^o)\underline{S}_{ij}\frac{(\underline{F}^2 - 2)}{\underline{v}_{ij}} \tag{22}$$

$$\Delta\overline{v}_{ij} = -\lambda_{\overline{v}}\frac{\partial \Omega(t)}{\partial \overline{v}_{ij}} = -\lambda_{\overline{v}}\frac{\partial \Omega(t)}{\partial u_o}\left(\frac{\partial u_o}{\partial \underline{S}_{ij}}\frac{\partial \underline{S}_{ij}}{\partial \overline{v}_{ij}} + \frac{\partial u_o}{\partial \overline{S}_{ij}}\frac{\partial \overline{S}_{ij}}{\partial \overline{v}_{ij}}\right) = \lambda_{\overline{v}}\sum_{o=1}^{n_o}(\overline{W}_{ijo}^a - \overline{W}_{ijo}^o)\overline{S}_{ij}\frac{(\overline{F}^2 - 2)}{\overline{v}_{ij}} \tag{23}$$

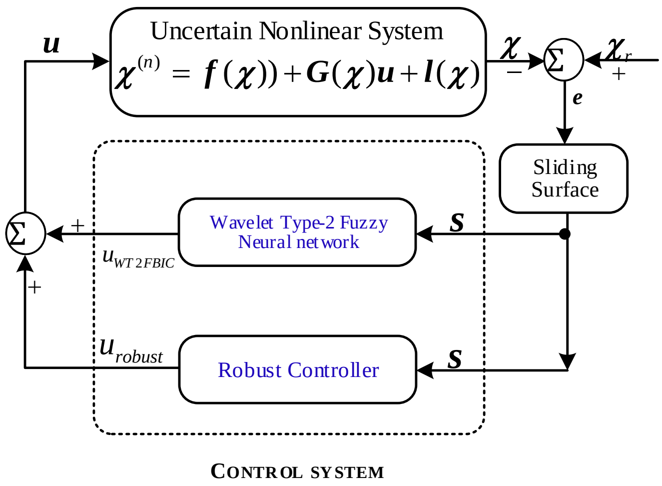

Figure 2. *Proposed control system diagram*

The proposed WT2FBIC is examined to mimic the ideal controller. The proposed control system is shown in Figure 2, which includes a main controller $\boldsymbol{u}_{\text{WT2FBC}}$ and a robust controller $\boldsymbol{u}_{robust}$ as follows

$$\boldsymbol{u}^* = \boldsymbol{u}_{\text{WT2FBIC}} + \boldsymbol{u}_{\text{robust}} \tag{24}$$

where $\boldsymbol{u}_{\text{robust}}$ is used for compensating the error between $\boldsymbol{u}^*$ and $\boldsymbol{u}_{\text{WT2FBIC}}$ to attain robust performance.

Defining the approximation error between $\boldsymbol{u}_{\text{WT2FBIC}}$ and $\boldsymbol{u}^*$ is $\boldsymbol{\theta}$.

$$\boldsymbol{\theta} = \boldsymbol{u}^* - \boldsymbol{u}_{\text{WT2FBIC}} \tag{25}$$

Defining the sliding surface as follows $\boldsymbol{s} = \boldsymbol{e} + \Psi\int edτ$. From (19), (20), (21), and (22), gets

$$\dot{\boldsymbol{s}} = \dot{\boldsymbol{e}} + \Psi\boldsymbol{e} = \boldsymbol{\theta} - \boldsymbol{u}_{\text{robust}} \tag{26}$$

Assuming the approximation error is bounded $0 \le \|\boldsymbol{\theta}\| \le \boldsymbol{\theta}_{\text{upper}}$, where $\boldsymbol{\theta}_{\text{upper}}$ is an upper bounded value of $\boldsymbol{\theta}$. The robust compensator is chosen as

$$\boldsymbol{u}_{\text{robust}} = \hat{\boldsymbol{\theta}}_{\text{upper}}\text{sign}(\boldsymbol{s}) \tag{27}$$

where $\hat{\boldsymbol{\theta}}_{\text{upper}}$ is an estimated value of $\boldsymbol{\theta}_{\text{upper}}$. And the adaptive law of $\hat{\boldsymbol{\theta}}_{\text{upper}}$ is given as

$$\hat{\boldsymbol{\theta}}_{\text{upper}} = \beta_{\theta}\|\boldsymbol{s}\| \tag{28}$$

Choosing a Lyapunov function as in (28), in which $\tilde{\boldsymbol{\theta}}_{\text{upper}} = \boldsymbol{\theta}_{\text{upper}} - \hat{\boldsymbol{\theta}}_{\text{upper}}$.

$$V = \frac{1}{2}\boldsymbol{s}^T\boldsymbol{s} + \frac{\tilde{\boldsymbol{\theta}}_{\text{upper}}^T\tilde{\boldsymbol{\theta}}_{\text{upper}}}{2\beta_{\theta}} \tag{29}$$

The derivate of V is achieved

$$\dot{V} = \boldsymbol{s}^T(\boldsymbol{\theta} - \boldsymbol{u}_{\text{robust}}) + \frac{\tilde{\boldsymbol{\theta}}_{\text{upper}}^T\dot{\tilde{\boldsymbol{\theta}}}_{\text{upper}}}{\beta_{\theta}} = \boldsymbol{s}^T(\boldsymbol{\theta}^T - \hat{\boldsymbol{\theta}}_{\text{upper}}\text{sign}(\boldsymbol{s})) + \frac{\tilde{\boldsymbol{\theta}}_{\text{upper}}^T\dot{\tilde{\boldsymbol{\theta}}}_{\text{upper}}}{\beta_{\theta}} = \boldsymbol{s}^T\boldsymbol{\theta} - \hat{\boldsymbol{\theta}}_{\text{upper}}\|\boldsymbol{s}\| + \frac{\tilde{\boldsymbol{\theta}}_{\text{upper}}^T\dot{\tilde{\boldsymbol{\theta}}}_{\text{upper}}}{\beta_{\theta}} \tag{30}$$

Because $\boldsymbol{\theta}_{\text{upper}} = \tilde{\boldsymbol{\theta}}_{\text{upper}} + \hat{\boldsymbol{\theta}}_{\text{upper}}$ is constant so $\dot{\tilde{\boldsymbol{\theta}}}_{\text{upper}} = -\dot{\hat{\boldsymbol{\theta}}}_{\text{upper}} = -\beta_{\theta}\|\boldsymbol{s}\|$, therefore:

$$\dot{V} = \boldsymbol{s}^T\boldsymbol{\theta} - \hat{\boldsymbol{\theta}}_{\text{upper}}\|\boldsymbol{s}\| - \left(\boldsymbol{\theta}_{\text{upper}} - \hat{\boldsymbol{\theta}}_{\text{upper}}\right)\|\boldsymbol{s}\| = -\left(\boldsymbol{\theta}_{\text{upper}} - \|\boldsymbol{\theta}\|\right)\|\boldsymbol{s}\| \le 0 \tag{31}$$

Since $\dot{V}$ is negative semi-definite, it gives that $\tilde{\boldsymbol{\theta}}_{upper}$ and $\boldsymbol{s}$ are bounded. Defining $\Psi = \left(\boldsymbol{\theta}_{\text{upper}} - \|\boldsymbol{\theta}\|\right)\|\boldsymbol{s}\| \le -\dot{V}$. Integrating Λ with respect to time, attains:

$$\int_0^t \Psi d\tau \le V(0) - V \tag{32}$$

Because $V(0)$ is constrained, $\dot{V}$ does not increase and bounded, so $\lim_{t\to\infty}\int_0^t \Psi(\tau)d\tau < \infty$ This suggests that in the event $t \to \infty$ then $s \to 0$. As a result, the proposed WT2FBIC control algorithm is sure to maintain its stability.

5. Simulation Results

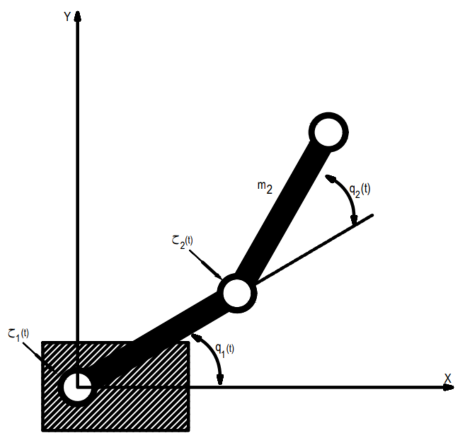

Figure 3. *Two joint robot manipulator.*

JTE HCMUTE
ISSN: 2615-9740
JOURNAL OF TECHNICAL EDUCATION SCIENCE
Ho Chi Minh City University of Technology and Education
Website: https://jte.edu.vn
Email: jte@hcmute.edu.vn

The diagram of two joint robot manipulator is shown in figure 3. The dynamic equation of 2 DOFs rigid manipulator is represented by Euler-Lagrange system as [11], [12], [13].

$$\begin{bmatrix}\tau_1\\ \tau_2\end{bmatrix}=\begin{bmatrix}(m_1+m_2)r_1^2+m_2r_2^2+2m_2r_1\,r_2\,c_2 & m_2r_2^2+m_2r_1\,r_2\,c_2\\ m_2r_2^2+m_2r_1\,r_2\,c_2 & m_2r_2^2\end{bmatrix}.\begin{bmatrix}\ddot{q}_1\\ \ddot{q}_2\end{bmatrix}+$$
$$+\begin{bmatrix}-m_2.r_1\,.r_2\,.s_2.(\dot{q}_1+\dot{q}_2)\dot{q}_1 & 0\\ 0 & m_2.r_1r_2\,.\dot{q}_2\end{bmatrix}\begin{bmatrix}\dot{q}_1\\ \dot{q}_2\end{bmatrix}+\begin{bmatrix}((m_1+m_2).l_1\,.c_2+m_2l_2c_{12}g\\ (m_2.l_2.c_{12})g\end{bmatrix}+\begin{bmatrix}d_1\\ d_2\end{bmatrix} \quad (33)$$

where $m_1,\ l_1,\ m_2,\ l_2$ denotes the mass and length of two links, respectively; $d_1,\ d_2$ denotes the disturbances to link 1 and link 2, respectively; $c_1=\cos(q_1),\ s_1=\sin(q_1),\ c_2=\cos(q_2),\ s_2=\sin(q_2), c_{12}=\cos(q_1+q_2)$. And the specification and initial values of the parameters of the robot system is shown in table 1 as below.

Table 1. *The details and initial points for the parameters of two- joint robot manipulator [13]*

Gravity constant	$g=9.81$ (m/s^2)
The torque of robot system	$\boldsymbol{u}=[\tau_1\ \tau_2]^T$
The disturbance	$\boldsymbol{d}=[d_1\ d_2]^T=[0.5\sin(t);\ 0.4\sin(t)]^T$
The mass of link 1 and link 2	m_1=1 (kg), m_2=1 (kg)
The angle position of robot system	$\boldsymbol{q}=[q_1\ q_2]^T$
Length of joints 1 and 2	$l_2=l_1=1\ (m)$
The half-length of joints 1 and 2	$r_2=0.5\times l_2,\ r_1=0.5\times l_1$
Command amplitude	Amp=(11.45*pi)/180
The combine effect of friction	$c_2=\cos(q_2),\ s_2=\sin(q_2), c_{12}=\cos(q_1+q_2)$.
The initial condition of q_1 and q_2	q_1=6*pi/180 (rad), $q_2(0)$=6*pi/180 (rad)
The initial condition of $\dot{q}_1$ and $\dot{q}_2$	$\dot{q}_1=0$, $\dot{q}_2=0$

Let we set

$D_{11}=(m_1+m_2)r_1^2+m_2r_2^2+2m_2r_1\,r_2\,c_2$

$D_{12}=D_{21}=m_2r_2^2+m_2r_1\,r_2\,c_2$

$D_{22}=m_2r_2^2$

$C_1=-m_2.r_1\,.r_2\,.s_2.(\dot{q}_1+\dot{q}_2)$

$C_2=m_2.r_1r_2\,.\dot{q}_2$

$g_1(q_1,q_2)=((m_1+m_2).l_1\,.c_2+m_2l_2c_{12}g$

$g_2(q_1,q_2)=(m_2.l_2.c_{12})g$

The equation (33) can be represented as follows.

$$\begin{bmatrix}\tau_1\\ \tau_2\end{bmatrix}=\begin{bmatrix}D_{11} & D_{12}\\ D_{21} & D_{22}\end{bmatrix}.\begin{bmatrix}\ddot{q}_1\\ \ddot{q}_2\end{bmatrix}+\begin{bmatrix}C_1 & 0\\ 0 & C_2\end{bmatrix}\begin{bmatrix}\ddot{q}_1\\ \ddot{q}_2\end{bmatrix}+\begin{bmatrix}g_1(q_1,q_2)\\ g_2(q_1,q_2)\end{bmatrix}+\begin{bmatrix}d_1\\ d_2\end{bmatrix} \quad (34)$$

The let we set:

JTE HCMUTE
ISSN: 2615-9740
JOURNAL OF TECHNICAL EDUCATION SCIENCE
Ho Chi Minh City University of Technology and Education
Website: https://jte.edu.vn
Email: jte@hcmute.edu.vn

$\boldsymbol{u}=\begin{bmatrix}\tau_1\\ \tau_2\end{bmatrix}$, $\boldsymbol{M}=\begin{bmatrix}D_{11} & D_{12}\\ D_{21} & D_{22}\end{bmatrix}$, $\ddot{\boldsymbol{\chi}}=\begin{bmatrix}\ddot{q}_1\\ \ddot{q}_2\end{bmatrix}$, $\boldsymbol{C}=\begin{bmatrix}C_1 & 0\\ 0 & C_2\end{bmatrix}$, $\dot{\boldsymbol{\chi}}=\begin{bmatrix}\dot{q}_1\\ \dot{q}_2\end{bmatrix}$, $\boldsymbol{d}=\begin{bmatrix}d_1\\ d_2\end{bmatrix}$, equation (34) becomes

$$\boldsymbol{u}=\boldsymbol{M}\ddot{\boldsymbol{\chi}}+\boldsymbol{C}\dot{\boldsymbol{\chi}}+\boldsymbol{d} \tag{35}$$

$$\Leftrightarrow \frac{1}{\boldsymbol{M}}\boldsymbol{u}=\ddot{\boldsymbol{\chi}}+\frac{\boldsymbol{C}\dot{\boldsymbol{\chi}}}{\boldsymbol{M}}+\frac{\boldsymbol{d}}{\boldsymbol{M}} \tag{36}$$

$$\Leftrightarrow \ddot{\boldsymbol{\chi}}=-\frac{\boldsymbol{C}\dot{\boldsymbol{\chi}}}{\boldsymbol{M}}+\frac{1}{\boldsymbol{M}}\boldsymbol{u}-\frac{\boldsymbol{d}}{\boldsymbol{M}} \tag{37}$$

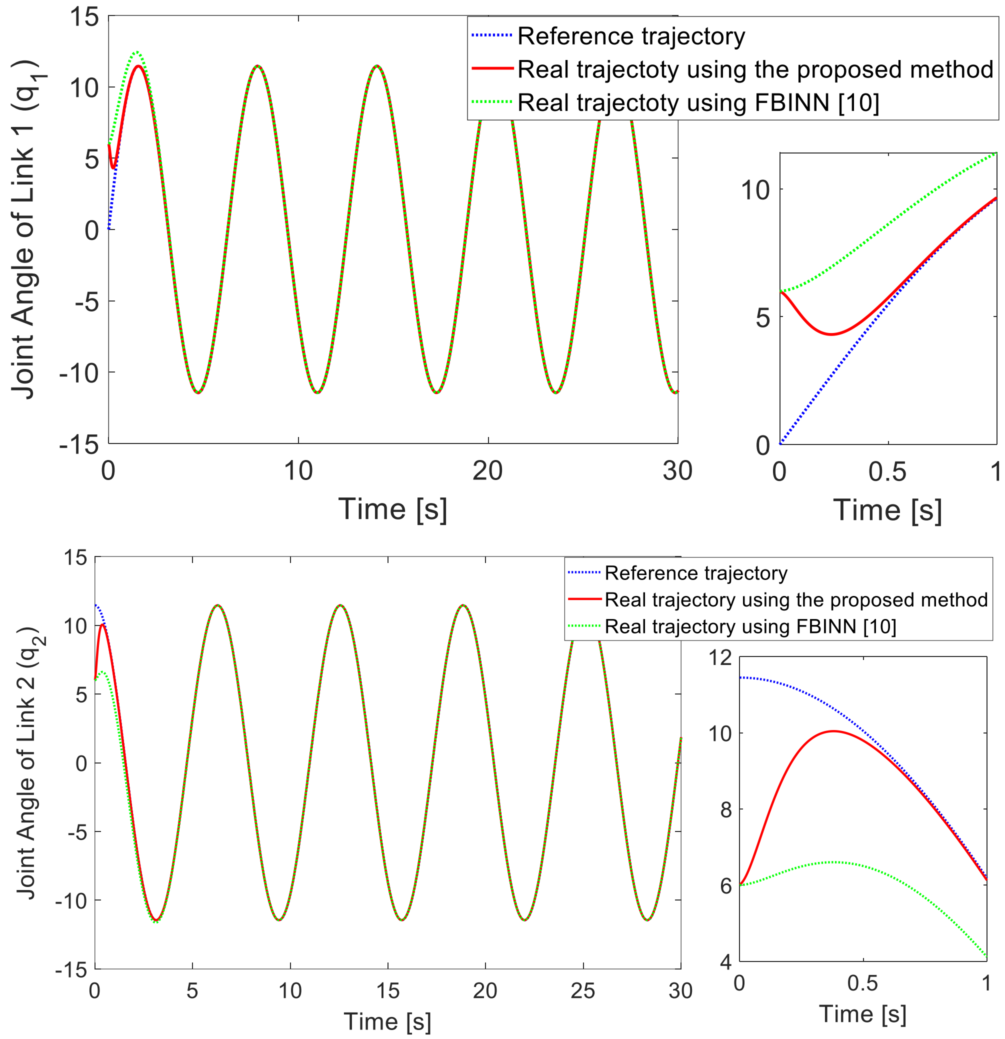

Figure 4. *The online trajectories tracking of joint 1 and joint 2 using proposed method.*

Table 2. *Comparison of other neural networks and our method*

Method	RMSE₁	RMSE₂	Average_RMSE
Brain imitated neural network [7]	0.311	0.3637	0.3373
Fuzzy brain imitated neural network [10]	0.2245	0.1358	0.1802
Our method	0.1857	0.1248	0.1552

JTE
HCMUTE
ISSN: 2615-9740

JOURNAL OF TECHNICAL EDUCATION SCIENCE
Ho Chi Minh City University of Technology and Education
Website: https://jte.edu.vn
Email: jte@hcmute.edu.vn

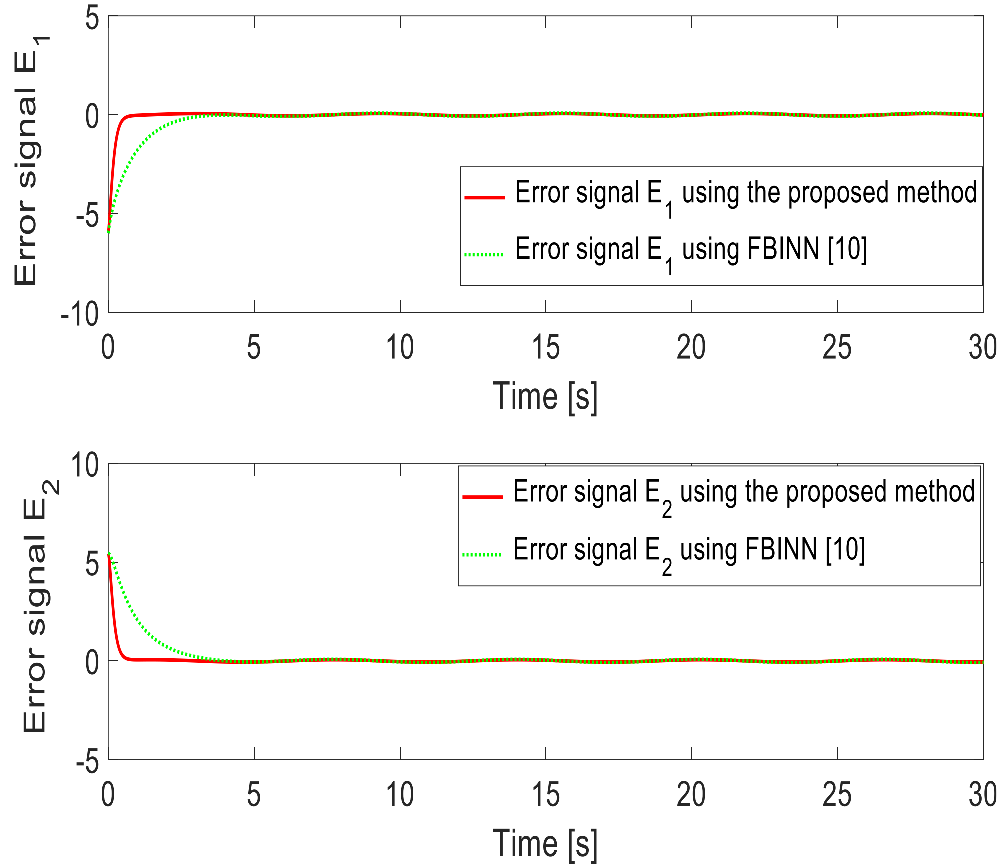

Figure 5. *The tracking error signals of joint 1 and joint 2 using proposed method.*

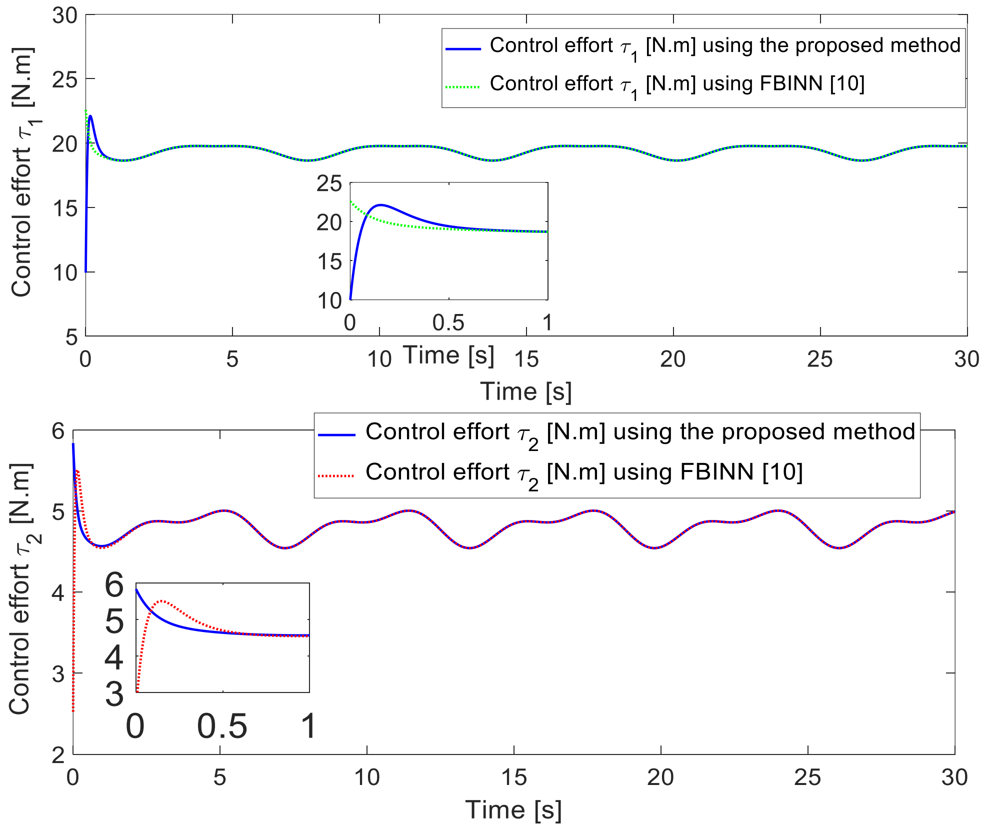

Figure 6. *The control efforts using proposed method.*

Let we set $\boldsymbol{f}(\chi)) = -\frac{\boldsymbol{C}\dot{\chi}}{\boldsymbol{M}}$, $\boldsymbol{G}(\chi) = \frac{1}{\boldsymbol{M}}$, $\boldsymbol{l}(\chi) = -\frac{\boldsymbol{d}}{\boldsymbol{M}}$ then equation becomes equation (1). So the proposed method can be applied for the robot system. And the initial values for the parameters of the proposed method are chosen as follows $\lambda_{\vartheta} = 0.001, \lambda_{\theta} = 0.001$, $\bar{W}_{ijo}^{a} = 0.1$, $\underline{W}_{ijo}^{a} = 0.05$, $\bar{W}_{ijo}^{o} = 0.1$, $\underline{W}_{ijo}^{o} = 0.05$, $n_j = 10,\ n_i = 2,\ n_o = 2$, $\mu_{ij} = 0.1, \underline{v}_{ij} = 0.2, \bar{v}_{ij} = 0.4$. The online trajectories of our method comparing with fuzzy brain imitated neural network FBINN [10] method are shown in Figure 5, the error signals are shown in figure 6 and control efforts is shown in Figure 7. In figure 5, the tracking output of the proposed method to the reference trajectory is better than the tracking output of FBINN [10]. Moreover, the error signal of our method comes to zero faster and stronger than the error signal of FBINN [10]. Finally, the RMSE (root-mean-squared error) of the proposed method is compared with the brain imitated neural network (BINN) [7] and fuzzy brain imitated neural network (FBINN) [10] in Table 2. The root mean square error (RMSE) of our method is 2.1733 times lower than that of the BINN [7] and 1.1611 times lower than that of the FBINN [10]. Compared to BINN and FBINN, our technique clearly performs better.

Conclusions

In this paper, a novel artificial neural network, the Wavelet Type-2 Fuzzy Brain Imitated Controller (WT2FBIC), is presented as a means to control nonlinear systems. You can ensure the stability of the system by implementing the proposed WT2FBIC-based control mechanism. Simulation tests have shown that a two-joint robot manipulator can achieve favorable control performance when using a system based on the WT2FBIC control protocol. This proves that the proposed approach works well with nonlinear systems. The main limitation of the proposed method is the learning rates, which are determined by trial and error. In the future, an optimization method called balancing composite motion optimization (BCMO) will be used to find the best optimal values for the learning rate.

Conflict of Interest

The author declares no conflict of interest.

REFERENCES

[1] R. Maity, R. Mishra, and P. K. Pattnaik, "A Review of Flying Robot Applications in Healthcare," P. K. Pattnaik, A. Vaidya, S. Mohanty, S. Mohanty, A. Hol, (eds) *Smart Healthcare Analytics: State of the Art. Intelligent Systems Reference Library*, vol. 213. Springer, Singapore, 2022.

[2] D. M. C. Gabriel, R. P. Marcelo, and P. M. António, "Augmented Reality for Human–Robot Collaboration and Cooperation in Industrial Applications: A Systematic Literature Review," *Sensors*, vol. 22, no. 7, p. 2725, 2022.

[3] B. V. Amsterdam, M. J. Clarkson and D. Stoyanov, "Gesture Recognition in Robotic Surgery: A Review," in *IEEE Transactions on Biomedical Engineering*, vol. 68, no. 6, pp. 2021-2035, June 2021.

[4] G. Garas *et al.*, "Novel strategies for managing retropharyngeal lymph node metastases in head and neck and thyroid cancer with Transoral Robotic Surgery (TORS)," *Annals of Surgical Oncology*, pp. 1-10, 2022.

[5] W. Huang, S. K. Oh, and W. Pedrycz, "Hybrid Fuzzy Wavelet Neural Networks Architecture Based on Polynomial Neural Networks and Fuzzy Set/Relation Inference-Based Wavelet Neurons," in *IEEE Transactions on Neural Networks and Learning Systems*, vol. 29, no. 8, pp. 3452-3462, Aug. 2018.

[6] C. Lucas, D. Shahmirzadi, and N. Sheikholeslami, "Introducing BELBIC: brain emotional learning based intelligent controller," *Intelligent Automation Soft Computing*, vol. 10, no. 1, pp. 11-21, 2004.

[7] C. M. Lin, D. H. Pham, and T. T. Huynh," Synchronization of chaotic system using a brain-imitated neural network controller and its applications for secure communications," *IEEE Access*, vol. 9, pp.75923-75944, 2021.

[8] C. M. Lin, D. H. Pham, and T. T. Huynh, "Encryption and Decryption of Audio Signal and Image Secure Communications Using Chaotic System Synchronization Control by TSK Fuzzy Brain Emotional Learning Controllers," in *IEEE Transactions on Cybernetics*, vol. 52, no. 12, pp. 13684-13698, Dec. 2022.

[9] D. Wu and J. M. Mendel, "Enhanced Karnik-Mendel Algorithms for Interval Type-2 Fuzzy Sets and Systems," NAFIPS 2007 - 2007 *Annual Meeting of the North American Fuzzy Information Processing Society*, San Diego, CA, USA, 2007, pp. 184-189.

[10] D. H. Pham, C. M. Lin, V. N. Giap, V. P. Vu, and H. Y. Cho, "Design of Missile Guidance Law Using Takagi-Sugeno-Kang (TSK) Elliptic Type-2 Fuzzy Brain Imitated Neural Networks," in *IEEE Access*, vol. 11, pp. 53687-53702, 2023.

[11] T. Q. Ngo, D. K. Hoang, T. T. Tran, T. T. Nguyen, V. T. Nguyen, and L. H. Le, "A novel self-organizing fuzzy cerebellar model articulation controller based overlapping Gaussian membership function for controlling robotic system," *International Journal of Computers Communications & Control*, vol. 17, no. 4, 2022.

[12] R. M. Murray, Z. Li, and S. S. Sastry, "A mathematical introduction to robotic manipulation," *CRC press*, 2017.

[13] V. T. Nguyen, C. Y. Lin, S. F. Su, W. Sun, and M. J. Er, "Global Finite Time Active Disturbance Rejection Control for Parallel Manipulators With Unknown Bounded Uncertainties," *IEEE Transactions on Systems, Man, and Cybernetics: Systems*, vol. 51, no. 12, pp. 7838-7849, Dec. 2021.

[14] D. H. Pham, T. T. Huynh, and C. M. Lin, "Fault-Tolerant Control for Robotic Systems Using a Wavelet Type-2 Fuzzy Brain Emotional Learning Controller and a TOPSIS-Based Self-organizing Algorithm," *Int. J. Fuzzy Syst.*, vol. 25, pp. 1727–1741, 2023.

JTE
HCMUTE
ISSN: 2615-9740

JOURNAL OF TECHNICAL EDUCATION SCIENCE
Ho Chi Minh City University of Technology and Education
Website: https://jte.edu.vn
Email: jte@hcmute.edu.vn

Pham Duc Hung was born in Hung Yen Province, Vietnam, in 1983. He received the B.S. degree in Automatic Control from Hanoi University of Science and Technology, Vietnam, in 2006, the M.S. degree in Automation from Hanoi University of Science and Technology, Vietnam, in 2011, and he received Ph.D. degree in the Department of Electrical Engineering, Yuan Ze University, Chung-Li, Taiwan, in 2022. He is also a Lecturer with Faculty Electrical and Electronic, Hung Yen University of technical and education, Vietnam. His research interests include fuzzy logic control, neural network, cerebellar model articulation controller, brain emotional learning-based intelligent controller, fault tolerant control, secure communication and robot control.

Email: duchung.pham@utehy.edu.vn. ORCID: https://orcid.org/0000-0003-3344-1593